Plasma surface modification of advanced organic fibres

Part I Effects on the mechanical, fracture and ballistic properties of aramid/epoxy composites

J. R. BROWN*, P. J. C. CHAPPELL, Z. MATHYS
Materials Research Laboratory, DSTO Melbourne, P.O. Box 50, Ascot Vale, Victoria 3032, Australia

A marked improvement in the interlaminar shear strength and flexural strength of aramid/ epoxy composites is observed when the fibres are pretreated in an ammonia or ammonia/ nitrogen gaseous discharge (plasma) to introduce amine groups on to the fibre surface. Scanning electron and optical microscopic observations are used to examine the microscopic basis for these results. Scanning electron micrographs of shear fracture surfaces show clean fibre/matrix separation in composites made from untreated fibres, indicative of weak interfacial bonding. In contrast, shear fracture surfaces of composites containing plasma-treated fibres exhibit clear evidence of fibre fibrillation and matrix cracking, suggesting stronger interfacial bonding. Optical microscopic examination of flexure specimens shows that enhanced strength results mainly from reduced compressive fibre buckling and debonding, due to an increase in fibre/matrix interfacial bond strength. This increase is not accompanied by any significant change in the interlaminar fracture energy or flexural modulus of the composites, but there is an appreciable loss in transverse ballistic impact properties. These results are also examined in terms of the observed increase in fibre/matrix interfacial strength.

1. Introduction

The use of advanced fibre-reinforced organic matrix composites has grown substantially in recent years. This has been due to major advances in composite mechanical properties which have resulted from the use of strong, high-modulus reinforcing fibres such as carbon, aramid and, more recently, polyethylene. At the same time, attention has been paid to the development of improved matrix materials as well as to chemical and other types of fibre surface modification to control fibre/matrix interfacial characteristics, in order to improve composite impact resistance or damage tolerance, fatigue life and environmental durability.

Fibre/matrix adhesion in advanced composites results from mechanical, physical or chemical interactions at the fibre/matrix interface, and considerable effort has been directed at characterizing the surface energetics of fibres and identifying relationships between wetting behaviour and interfacial bond strengths [1-5]. A variety of fibre surface treatment and modification techniques has been developed to improve interfacial bonding and to enhance fibre processability. Aramid fibre-reinforced composites are characterized by a relatively low fibre/matrix interfacial strength and the primary aim in improving interfacial bonding has been to maximize filament

wettability, with chemical bond formation as a secondary objective. This has involved both etching [6] and chemical modification [7-10] of the filament surface. The improvements in interlaminar properties achieved by more aggressive treatments [7, 8] have been accompanied by substantial losses in filament strength. However, milder chemical treatments [9, 10] and ammonia or monomethylamine plasma treatments [11, 12] have resulted in significant improvements in interlaminar properties of aramid composites without accompanying mechanical degradation of the filaments. Despite this success, however, there is conflicting evidence about the relative contributions of chemical interactions (principally covalent chemical bonding) and physical interactions (dispersive forces, dipole–dipole interactions, or acid–base interactions) to improvements in interlaminar properties.

Also of interest in fibre-reinforced composites is the relationship between the microscopic deformation and failure processes which occur at the fibre/matrix interface, and the interlaminar and tensile properties of the material. Flexural properties depend primarily on the tensile, compressive and shear properties of the reinforcing fibres and, to a lesser extent, those of the matrix, as well as the fibre/matrix interfacial bond strength. The transverse ballistic impact properties are also determined mainly by the fibre tensile modulus

---

* Author to whom all correspondence should be addressed.

and strength, and the level of interfacial bonding. The interlaminar shear strength is governed by the shear properties of the composite components and interface while the interlaminar fracture energy (both tensile and shear failure modes) depends predominantly upon matrix fracture energy and to varying degrees upon crack branching and fibre bridging across crack faces, fibre pull-out and interfacial bond strength [13, 14]. While improved bonding between fibre and matrix results in more efficient stress transfer at the interface, the extent to which composite tensile and interlaminar properties are affected is difficult to estimate.

This paper considers the chemical aspects of treatment of aramid fibres in ammonia or ammonia/nitrogen plasmas to introduce surface amine groups, the response of tensile and interlaminar properties (shear strength, flexural modulus, flexural strength, fracture energy and ballistic impact resistance) of aramid/epoxy composites to the surface treatment, and the microscopic basis for failure in these composites.

2. Materials and techniques

2.1. Aramid fabric
Aramid fabric (Kevlar® 49, style 352, 1150 denier) was obtained from Du Pont (Australia) Ltd. The fabric was woven and scoured by Clark–Schwebel Fiber Glass Corp. Because commercially scoured Kevlar 49 has residual processing aids on the fibre surface [1, 2], the fabric was cleaned by Soxhlet extraction in water and then acetone, and dried for 24 h at 105 °C before further use.

2.2. Plasma surface treatment of aramid fabric
Plasma treatments were carried out with ammonia in a Plasmaprep 500XP plasma reactor. The plasma was generated by a 13.56 MHz capacitively coupled discharge in a cylindrical chamber 23 cm long and 21 cm diameter. Fabric samples of 20 cm × 40 cm were mounted on a Perspex® rack in the chamber, which was evacuated to a pressure of 10^{-4} torr (1 torr = 1.333 × 10² Pa) prior to the admission of the ammonia. A reactor power of 100 W, a pressure of 0.25 torr and a gas flow rate of 20 standard cm³ min⁻¹ were used for the plasma treatment. In an attempt to increase the degree of reaction, without resorting to excessive reaction times and power, a mixed ammonia/nitrogen plasma with a flow rate of 10 standard cm³ min⁻¹ for each component gas was also used. After plasma treatment the samples were left in flowing gas for 15 min before the chamber was evacuated and air admitted, in order to allow for the decay of residual surface radicals.

2.3. Chemical characterization of plasma-treated fabric
Plasma treatment in ammonia or ammonia/nitrogen results in the incorporation of amine groups on to the aramid fibre surface. The surface concentration was measured by dye assay, using the technique described by Allred [12]. Briefly, amine groups on the fibre surface were protonated by acid treatment, and the

counter anion was exchanged for the dye anion. The bound dye was then eluted with a base and its concentration determined spectrophotometrically. The azo-sulphonate dye Crocein Orange G (CI 15970, Sigma Chemicals C-3268) was chosen because it has only one binding site and is available in relatively high purity. Dye concentrations were measured using the absorption maximum at 480 nm.

The number of surface amine groups per square nanometre (nm²), N, is given by

$$N = \frac{6.023C}{MWA} \qquad (1)$$

where M is the molecular weight of the dye, W is the weight of the fabric sample (g), C is the dye concentration (p.p.m.) in a 10 cm³ sample, and A is the specific surface area of the fibre (m² g⁻¹). The specific surface area was calculated to be 0.233 m² g⁻¹ for the 11.9 μm diameter aramid fibres (density 1.44 g cm⁻³).

2.4. Aramid/epoxy composite fabrication
Aramid/epoxy composites were fabricated from both untreated and plasma-treated fabrics and the diglycidyl ether of bisphenol A (DGEBA) (Shell Epon 828) and diaminodiphenyl methane (DDM) [15]. Fibre treatment times are given in Table I. The fabrics were impregnated by passing samples through a solution containing 120 g DGEBA, 32.4 g DDM and 234 g methyl ethyl ketone. The solvent was removed by initial evaporation at room temperature for 30 min and then at 80 °C for a further 15 min. The impregnated fabric composites (20 plies) were cured for 2 h at 80 °C and 2 h at 120 °C at a pressure of 350 kPa. The matrix content was nominally 33% by weight. Individual values are listed in Table I.

2.5. Interlaminar shear strength
The interlaminar shear strength of the composites was determined using the four-point shear test method of Browning et al. [16]. Specimen dimensions were nominally 50 mm × 10 mm × 4 mm, with a span to depth ratio of 11.5. Specimens were conditioned at 23 °C and 50% relative humidity for 24 h before testing in an Instron testing machine at a crosshead speed of 2 mm min⁻¹.

The interlaminar shear strength, T, for the four-point test is given by the expression

$$T = \frac{3P}{4bd} \qquad (2)$$

where P is the failure load, b is the beam width and d is the beam depth.

2.6. Flexural properties
The flexural modulus and flexural strength of the composites were determined in accordance with standard flexure test procedures [17] using a three-point loading system and support span length/depth (L/d) ratios recommended by Zweben et al. [18]. Modulus specimens were tested at $L/d = 60$ and 32.

Plasma treatment	Matrix content (wt %)	Interlaminar shear strength (MPa)	Flexural modulus (GPa)	Flexural strength (MPa)	Interlaminar fracture energy ($J\,m^{-2}$)
None	33.6	24.2 ± 0.4 (9 samples)	31.0 ± 0.7	305 ± 16	587 ± 59 (5 samples)
Ammonia (30 s)	32.8	30.9 ± 0.5 (6 samples)	32.5 ± 1.1	421 ± 18	522 ± 63 (4 samples)
Ammonia (5 min)	32.6	33.2 ± 1.2 (5 samples)	32.5 ± 0.8	442 ± 18	539 ± 98 (6 samples)
Ammonia/nitrogen (5 min)	32.3	29.4 ± 2.3 (5 samples)	31.5 ± 1.3	390 ± 19	619 ± 81 (4 samples)

For $L/d = 60$, specimens nominally 300 mm × 13 mm × 4 mm with a span of 240 mm were tested at a speed of 20 mm min^{-1}. For $L/d = 32$, specimens nominally 150 mm × 13 mm × 4 mm with a span of 128 mm were tested at a speed of 5 mm min^{-1}. The flexural strength was measured by testing the modulus specimens with $L/d = 32$ to failure at a speed of 5 mm min^{-1}.

The flexural modulus (tangent modulus of elasticity), E_B, and the flexural strength, were calculated from the relationships

$$E_B = \frac{L^3 m}{4bd^3} \tag{3}$$

$$S = \frac{3PL}{2bd^2} \tag{4}$$

where L is the length of the support span, m is the slope of the initial linear portion of the load–deflection curve, and P, b and d are defined as above.

2.7. Interlaminar fracture energy

The opening mode (Mode I) interlaminar fracture energy or critical strain energy release rate, G_{Ic}, was determined by the compliance method using double cantilever beam (DCB) test specimen geometry [19, 20]. The general expression for G_{Ic} is

$$G_{Ic} = \frac{P_c^2}{2b} \frac{dC}{da} \tag{5}$$

where P_c is the load required to extend a crack of length a in a specimen of thickness b, and C is the specimen compliance. The compliance method is based upon the beam theory assumption that each half of the DCB specimen behaves as a cantilever beam in which C is given by

$$C = ka^3 \tag{6}$$

where k is a constant for a particular test specimen and is determined by fitting a third-order power curve to experimental C versus a values.

Beam specimens of dimensions 57 mm × 14.5 mm × 4 mm containing mid-ply starter cracks at one end were cut from composite panels. The starter cracks were produced by partially inserting a 0.075 mm thick layer of Teflon film between the mid-plies during composite lay-up. The test method requires a transverse tensile load to be applied at the beam end containing the starter crack. This was accomplished

by adhesively bonding P-shaped aluminium end-tabs containing loading holes to the upper and lower composite surfaces, so that the loading line coincided with the specimen end. Specimens were tested at a cross-head speed of 1 mm min^{-1}. The load-point crack opening displacement (COD) was recorded using an extensometer with a gauge length of 5 mm. For each treatment, specimens with various length starter cracks were loaded elastically and C was measured from the load, P, versus COD curves. The crack was extended by a few millimetres in each of a series of loading/unloading cycles, and its length from the load line was measured using a travelling microscope.

Although beam theory assumes the cubic relationship given in Equation 6, Berry [21] and Russell [22] have used an empirical nth order power curve and a third-degree polynomial, respectively, to relate C and a for composite materials. In order to calculate G_{Ic} values from the interlaminar fracture experiments, the most appropriate model for fitting the compliance versus crack length data (power curve or polynomial curve), was determined from plots of log(compliance) as a function of log(crack length). The plots obtained were linear (an example is shown in Fig. 1) and consequently a power fit was used.

2.8. Ballistic impact properties

The transverse ballistic impact properties were determined using the Materials Research Laboratory gas-gun facility [23] and 17 grain fragment-simulating
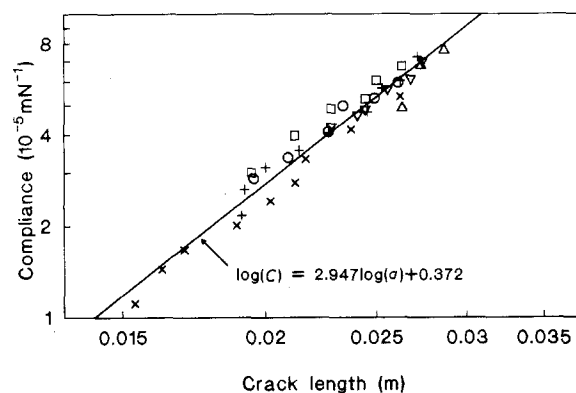
Figure 1 Plot of log(compliance) versus log(crack length) for a series of untreated aramid/epoxy composite specimens (each symbol refers to a specific specimen with a different starter crack length).

projectiles [24]. The V_{50} data (projectile velocity at which the probability of target penetration is 50%) were determined according to the procedures of MIL-STD-662 E [25].

2.9. Fracture surface examination
The fracture surfaces were coated with gold, and were examined in a Cambridge S250 Stereo-scan Mark 2 scanning electron microscope (SEM) using secondary electrons.

3. Results and discussion
3.1. Plasma surface amination of aramid fabrics
Cleaned aramid fabric was plasma-treated in ammonia for times ranging from 0.25–20 min. The number of amine groups incorporated on to the fibre surface increases rapidly to a value of 0.4 groups/nm^2 after a 30 s treatment time. Beyond this time, the degree of surface amination increases more slowly (Fig. 2). Treatment in a mixed ammonia/nitrogen plasma instead of an ammonia plasma increases the degree of surface amination, e.g. for a treatment time of 5 min, the surface amine concentration increased from 0.56–0.71 groups/nm^2 for the chosen reactor conditions.

3.2. Interlaminar shear strength
The interlaminar shear strength of the aramid/epoxy composites was calculated using Equation 2. The results in Table I show that ammonia plasma treatment of aramid fibres for 30 s (surface concentration of 0.4 amine groups/nm^2) results in a 28% increase in interlaminar shear strength. Fibre treatment for 5 min (0.56 amine groups/nm^2) results in a further 10% increase in composite interlaminar shear strength. The higher level of surface amine groups (0.71 groups/nm^2) generated by treatment in a mixed ammonia/nitrogen plasma does not result in further improvement. The increase in interlaminar shear strength after plasma treatment of the aramid fibres is due to an increase in the fibre/matrix interface strength. There is clear evidence of this in the fracture surfaces shown in Fig. 3.
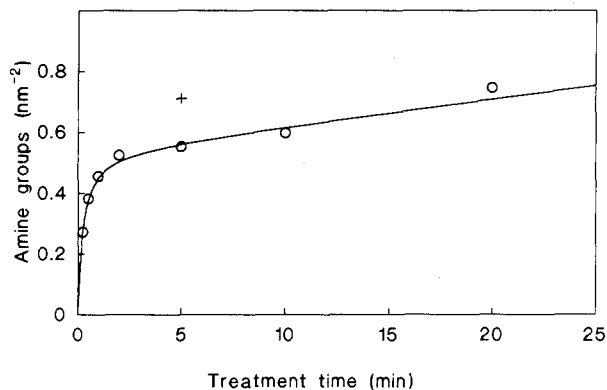
Figure 2 Degree of aramid fibre surface amination as a function of treatment time. (○) ammonia plasma, (+) ammonia/nitrogen plasma.

With untreated fibres, the composite has failed at the fibre/matrix interface, while with ammonia plasma-treated fibres this is no longer the dominant failure mode, and the composite has experienced additional shear failure within the fibre and the matrix. The interlaminar shear strength results are in general accord with the work of Stoller and Allred [26], who observed similar effects of ammonia plasma treatment of aramid fibre surfaces in T-peel experiments on two-ply laminates. The interfacial bond strength was shown to increase with surface amine concentration up to about 0.8 amine groups/nm^2, after which there was no further increase.

3.3. Flexural properties
Fig. 4 shows typical three-point flexure load versus deflection curves for composites containing untreated aramid fibres (a) and ammonia or ammonia/nitrogen plasma treated fibres (b). All materials exhibited similar linear load–deflection behaviour up to a load of about 150 N. Flexural modulus values were calculated from the slopes of the linear elastic portions of the load–deflection curves using Equation 3 and are presented in Table I. It is evident from Fig. 4 and from Table I that plasma treatment of the fibres has no significant effect on the flexural modulus of the resulting composite. This result confirms the general expectation that the flexural modulus is determined primarily by the tensile and compressive properties of the fibre and matrix, rather than by interfacial properties. However, work by Zweben et al. [18] suggests that care should be taken in determining the flexural modulus of composite specimens. In particular, if the L/d ratio is too low, the beam deflection may contain shear as well as bending components, giving an apparent flexural modulus lower than the true flexural modulus. In order to investigate the effect of L/d ratio on apparent flexural modulus, experiments were carried out for two different values of L/d, 32 and 60. The flexural modulus results in Table I are for $L/d = 60$. The results for $L/d = 32$ were approximately 2.5 GPa lower, suggesting a small shear contribution to the beam deflection at $L/d = 32$ and an even smaller contribution at $L/d = 60$.

The load–deflection behaviour of all specimens became non-linear above loads of 150 N, but composites made from untreated fibres and treated fibres behaved quite differently (see Fig. 4). Specimens made from untreated fibres started to fail at relatively low deflections, although they did not fail catastrophically until much higher deflections. However, with composites made from plasma-treated fibres, the load continued to increase until catastrophic failure took place. The flexural strengths of the composite specimens were calculated from the maximum loads using Equation 4 and are presented in Table I. These results show an increase of about 38% after 30 s plasma treatment of the fibres and about 45% after 5 min treatment. As for the interlaminar shear strength, there is no significant difference between the ammonia and ammonia/nitrogen plasma treatments. While the numerical values of flexural properties in three-point loading of a
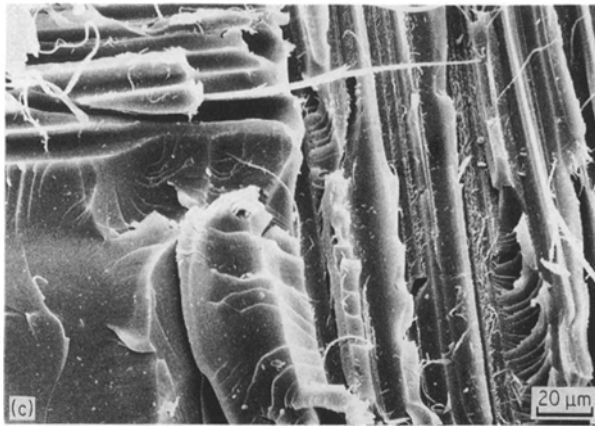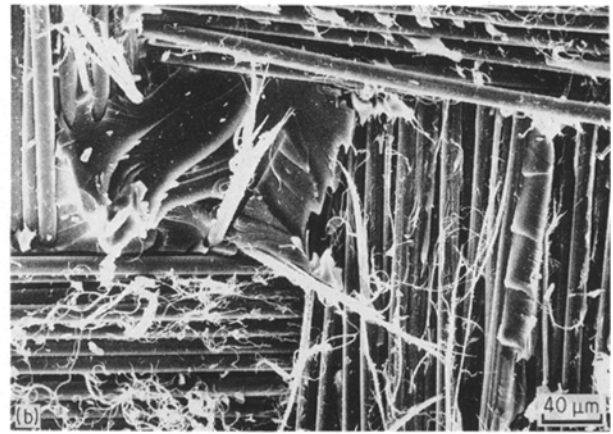
Figure 3 Interlaminar shear fracture surfaces of aramid/epoxy composites made from (a) untreated fibres, showing clean fibre/matrix separation, (b) ammonia plasma-treated fibres, showing fibre fibrillation, and (c) ammonia plasma-treated fibres, showing matrix cracking.

rectangular composite beam are readily determined by standard experimental procedures, the mechanism of flexural failure is more difficult to ascertain. In general, it is a complex process in which tensile, compressive and shear failure modes may be induced to varying degrees in each of the composite phases. Non-linearity in flexural load–deflection behaviour of aramid fibre-reinforced composites has been observed in extensive studies by Zweben [18, 27] and Allred [28, 29]. It is believed to be due to compressive failure in the flexural test specimens. It has been shown that the compressive stress–strain curves of unidirectional aramid/epoxy composites are strongly non-linear [27] and that the compressive strength is only about 20% of the tensile strength [30, 31]. The latter has been attributed to a buckling or kinking failure in the

Figure 4 Plot of load as a function of beam deflection for aramid/epoxy composites made from (a) untreated fibres and (b) ammonia plasma-treated fibres.

aramid fibres [30] or to a combination of low fibre compressive strength and a low fibre/matrix interfacial strength [31].

Microscopic examination of the failure modes in flexural test specimens made from untreated and plasma-treated fibres shows that the former contain more extensive fibre buckling and debonding which extend further into the composite from the compression surface. Both sets of specimens also failed on the tensile surface at maximum strain. Microscopic examination of the tensile surface showed matrix cracking and fibre/matrix debonding along fibres transverse to the tensile stress direction. These results indicate that the enhanced flexural strength of plasma-treated fibre composites occurs mainly as a result of a decrease in the extent of compressive fibre buckling, which is, in turn, due to increased fibre/matrix interfacial bonding.

3.4. Interlaminar fracture energy

The G_{Ic} values for the untreated and plasma-treated aramid/epoxy composites, determined using Equation 4, are presented in Table I. The exponents for the compliance versus crack length fits were found to be in the range 2.5–3.0 and the results show that there is no significant change in interlaminar fracture energy after fibre surface modification.

It has been established that composite interlaminar fracture energy is sensitive to and governed by the fracture toughness of the matrix resin up to a limiting resin toughness, beyond which the interlaminar fracture energy does not increase in the same proportion as that of the matrix [32–34]. This has been attributed to the limitation imposed on the resin deformation zone by the composite fibre plies. However, the extent to which composite interlaminar fracture energy is dependent upon the fibre/matrix interfacial properties is much less certain. Marom *et al.* [35] measured the G_{Ic} values of carbon and aramid fibre composites containing the same epoxy matrix and attributed a higher value of G_{Ic} for the carbon/epoxy composite

to its higher interfacial bond strength. However, Alesi et al. [36] studied interlaminar fracture of aramid/vinylester and aramid/polyester composites in which the aramid fabric had been surface treated to modify the interfacial properties, and found that G_{Ic} was governed almost entirely by the matrix resin properties with only a marginal contribution from interfacial properties.

In the present work, scanning electron micrographs of the DCB fracture surfaces of untreated fibre composites showed that fracture occurred predominantly in the matrix, with only small areas of fibre/matrix separation. A similar predominance of matrix failure was observed in fracture surfaces of composites made from treated fibres, and in those areas where delamination at the fibre/matrix interface was observed, there was increased evidence of fibre fibrillation, in accord with a higher fibre/matrix interfacial bond strength. However, it is clear from the similar G_{Ic} values for the treated and untreated fibre composites that the fibre/matrix interfacial bond strength is only a minor contributor to G_{Ic}.

precise mechanisms involved are not yet clearly understood. It is widely recognized that the ballistic performance of aramids is higher in the form of flexible fabric than in a reinforced resin composite [37, 38], and that those resin systems which promote composite mechanical and interfacial properties diminish the ballistic properties. For example, the flexural, compressive and interlaminar shear properties of aramid/epoxy composites are superior to those of aramid/polyester or aramid/vinylester composites, while the ballistic properties are inferior [39] (Table III). It has also been established that addition of low-energy fibre finishes or sizing, which reduce fibre/matrix adhesion and hence mechanical properties, enhances ballistic resistance by promoting energy absorption via fibre debonding and delamination [36, 40]. The results presented in Tables I and II, which show that fibre treatment in an ammonia plasma enhances the flexural and interfacial shear strength in aramid/epoxy composites while significantly decreasing the ballistic properties, are consistent with previous work.

3.5. Ballistic impact properties

The V_{50} ballistic limits of composites from untreated, ammonia plasma- and ammonia/nitrogen plasma-treated aramid fibres are given in Table II, together with their areal densities (20 plies) and resin contents. For composites containing nominally constant amounts of epoxy resin (32.5% by weight) a 30 s fibre treatment by ammonia plasma diminishes the composite ballistic performance against 17 grain fragment-simulating projectiles by 9.5%. A 5 min fibre treatment in either ammonia or ammonia/nitrogen lowers the ballistic properties by an additional 3%–4.5%.

Factors which influence the resistance of aramid composites to penetration on ballistic impact and the

4. Conclusions

Ammonia plasma treatment of aramid fibres results in changes in interface sensitive mechanical properties of aramid epoxy composites. Marked increases in the interlaminar shear and flexural strengths and a significant decrease in ballistic resistance are related to the introduction of surface amine groups which enhance the interaction between the fibres and the epoxy matrix, resulting in changes in composite failure mechanisms. The interlaminar shear results are in accord with SEM examinations of fracture surfaces which show clean fibre/matrix separation in the untreated fibre composites and fibre fibrillation and matrix fracture in composites containing treated fibres. Optical

TABLE II Ballistic impact properties of aramid/epoxy composites

Plasma treatment	Matrix content (wt %)	Areal density $(kg\,m^{-2})$	V_{50} ballistic limit $(m\,s^{-1})$	V_{50}/areal density $[(m\,s^{-1})/(kg\,m^{-2})]$
None	33.2	5.27	311 ± 12	59.0
Ammonia (30 s)	34.1	5.34	285 ± 9	53.4
Ammonia (5 min)	31.4	5.13	260 ± 10	50.7
Ammonia/nitrogen (5 min)	31.5	5.14	265 ± 17	51.6

TABLE III Effect of matrix resins on the mechanical and ballistic properties of Kevlar® aramid composites[a]

Resin type	Flexural modulus (GPa)	Flexural strength (MPa)	Compressive strength (MPa)	Interlaminar shear strength (MPa)	V_{50} ballistic limit[b] $(m\,s^{-1})$
Epoxy	30.3	310	138	30.5	280
Polyester	31.0	228	117	20.7	320
Vinylester	31.0	241	117–138	21.4	323

[a] Resin content 35%, areal density $9.28\,kg\,m^{-2}$. Data are taken from [39].
[b] 64 grain fragment-simulating projectile.

microscopic examination of test specimens shows that the increased flexural strength of treated fibre composites can be attributed to a lower degree of compressive fibre buckling due to enhanced interfacial bonding. The flexural modulus and interlaminar fracture energy are unchanged by plasma treatment. The flexural modulus results reflect the dependence of flexural modulus on tensile and compressive properties of the fibres, with only a small contribution from the fibre/matrix interface properties. The interlaminar fracture results are in accord with SEM examinations of fracture surfaces showing clear evidence of predominantly matrix failure in both untreated and treated fibre composites.

Acknowledgements

References

1. P. J. C. CHAPPELL and D. R. WILLIAMS, *J. Colloid Interface Sci.* **128** (1989) 450.
2. P. J. C. CHAPPELL and D. R. WILLIAMS, *J. Adhes. Sci. Technol.* **4** (1990) 7.
3. J. SCHULTZ, L. LAVIELLE and C. MARTIN, *J. Adhesion* **23** (1987) 45.
4. L. S. PENN, F. A. BYSTRY and H. J. MARCHIONNI, *Polym. Compos.* **4** (1983) 26.
5. L. T. DRZAL, in "Epoxy Resins and Composites II", edited by K. Dusek (Springer-Verlag, Berlin, 1986) pp. 1–32.
6. M. BREZNICK, J. BANJABI, H. GUTTMANN and G. MAROM, *Polym. Commun.* **28** (1987) 55.
7. T. S. KELLER, A. S. HOFFMAN, B. D. RATNER and B. J. McELROY, in "Physicochemical Aspects of Polymer Surfaces", Vol. 2, edited by K. L. Mittal (Plenum, New York, 1983) pp. 861–79.
8. Y. WU and G. C. TESORO, *J. Appl. Polym. Sci.* **31** (1986) 1041.
9. L. S. PENN, T. J. BYERLEY and T. K. LIAO, *J. Adhesion* **23** (1987) 163.
10. L. S. PENN, G. C. TESORO and H. X. ZHOU, *Polym. Compos.* **9** (1988) 184.
11. M. R. WERTHEIMER and H. P. SCHREIBER, *J. Appl. Polym. Sci.* **26** (1981) 2087.
12. R. E. ALLRED, PhD thesis, Massachusetts Institute of Technology (1983) pp. 39, 130, 131.
13. J. M. SCOTT and D. C. PHILLIPS, *J. Mater. Sci.* **10** (1975) 551.
14. A. J. RUSSELL and K. N. STREET, in "Proceedings of the 4th International Conference on Composite Materials", Tokyo, 25–28 October 1982, edited by T. Hayashi, K. Kawata and S. Umekawa (Japan Society for Composite Materials, Tokyo, 1982) p. 279.
15. T. F. MIKA, in "Epoxy Resins: Chemistry and Technology", edited by C. A. May and Y. Tanaka (Marcel Dekker, New York, 1973) p. 257.
16. C. E. BROWNING, F. L. ABRAMS and J. M. WHITNEY, ASTM STP 797 (American Society for Testing and Materials, Philadelphia, 1983) p. 54.
17. ASTM D 790-86, "Standard Test Methods for Flexural Properties of Unreinforced and Reinforced Plastics and Electrical Insulating Materials" (American Society for Testing and Materials, Philadelphia, 1986).
18. C. ZWEBEN, W. S. SMITH and M. W. WARDLE, ASTM STP 674 (American Society for Testing and Materials, 1978) p. 228.
19. A. J. SMILEY and R. B. PIPES, *J. Compos. Mater.* **21** (1987) 670.
20. J. M. WHITNEY, C. E. BROWNING and W. HOOGSTEDEN, *J. Reinf. Plastics Compos.* **1** (1982) 297.
21. J. P. BERRY, *J. Appl. Phys.* **34** (1963) 62.
22. A. J. RUSSELL, in "Factors Affecting the Opening Mode Delamination of Graphite/Epoxy Laminates", Materials Report 82-Q (Defence Research Establishment Pacific, Victoria, BC, Canada, 1982).
23. J. R. BROWN, P. J. C. CHAPPELL, G. T. EGGLESTONE and E. P. GELLERT, *J. Phys. E Sci. Instrum.* **22** (1989) 771.
24. MIL-P-46593A (ORD), Military Specification, "Projectile, Calibres 0.22, 0.30, 0.50 and 20 mm Fragment-Simulating", October 1962.
25. MIL-STD-662E. Military Standard, "V_{50} Ballistic Test for Armor", January 1987.
26. H. M. STOLLER and R. E. ALLRED, in "Proceedings of the 18th International SAMPE Technical Conference", Seattle, WA, 7–9 October 1986, edited by J. T. Hoggett, S. G. Hill and J. C. Johnson (SAMPE, Seattle, 1986) p. 993.
27. C. ZWEBEN, *J. Compos. Mater.* **12** (1978) 422.
28. R. E. ALLRED, *ibid.* **15** (1981) 100.
29. *Idem, ibid.* **15** (1981) 117.
30. J. H. GREENWOOD and P. G. ROSE, *J. Mater. Sci.* **9** (1974) 1809.
31. S. V. KULKARNI, J. S. RICE and B. W. ROSEN, *Composites* **6** (1975) 217.
32. W. D. BASCOM, J. L. BITNER, R. J. MOULTON and A. R. SIEBERT, *ibid.* **11** (1980) 9.
33. W. M. JORDAN and W. L. BRADLEY, ASTM STP 937 (American Society for Testing and Materials, Philadelphia, 1987) p. 95.
34. D. L. HUNSTON, *Compos. Tech. Rev.* **6** (1984) 176.
35. G. MAROM, I. ROMAN, H. HAREL, M. ROSENSAFT, S. KENIG and A. MOSHONOV, *Int. J. Adhes. Adhesives* **8** (1988) 85.
36. A. L. ALESI, J. R. BROWN and W. E. HASKELL III, in "Aramid Composite Structural Armor Materials for Ground Combat Vehicles", U.S. Army Materials Technology Laboratory Report MTL TR89-102, 1989.
37. R. G. SHEPHARD, in "Proceedings of the International Conference on Polymers in Defence", Bristol, UK, 18–20 March 1987 (The Plastics and Rubber Institute, London, 1987) p. 21/1.
38. G. M. SAVAGE, *Metals Mater.* **5** (1989) 285.
39. DuPont Publication, "Lightweight Protective Armor of Kevlar® Aramid", 1982.
40. D. R. HARTMAN, in "Proceedings of the 41st Annual Conference, Reinforced Plastics/Composites Institute", The Society of the Plastics Industry, 27–31 January 1986 (The Society of the Plastics Industry, New York, 1986) p. 16-D/1.